Natural Convection Heat Transfer with Molten Salt in a Differentially-Heated Cavity

Noah LeFrancois*, Jovan Nedic, and Melanie Tetreault-Friend
Department of Mechanical Engineering
McGill University
Montreal QC, H3A 2K7, Canada
noah.lefrancois@mail.mcgill.ca; jovan.nedic@mcgill.ca; melanie.tetreault-friend@hatch.com

ABSTRACT

Natural convection is an important mode of heat transfer in the design of passive safety systems for molten salt reactors. While heat transfer correlations for natural convection in water have been widely studied, there is a lack of equivalent experimental data for molten salts. An experimental investigation of convective heat transfer in a differentially-heated cavity using nitrate salts is presented in this paper with the goal of obtaining empirical heat transfer correlations which can be compared to existing correlations. Temperature distributions in the salt and on the cavity boundaries are measured using a combination of infrared thermometry and thermocouple probes, then one-dimensional heat transfer models are used to calculate the total heat flux and heat transfer coefficient. The Nusselt numbers observed for a $NaNO_3$-KNO_3 mixture were found to agree well with existing correlations, in contradiction to previous findings on nitrate mixtures with higher Prandtl number. Along with a significant Pr-dependence obtained for the observed data, this finding highlights the need for high-quality data to ensure confidence in the accuracy and range of applicability of Nusselt number correlations in order to inform the design of molten salt systems in advanced reactor technologies.

KEYWORDS
Molten Salts, Natural Convection, Differentially-Heated Cavity, Infrared Thermometry

1. INTRODUCTION

A major feature of Gen IV reactor design is the shift from active to passive cooling. Passive safety systems provide major advantages compared to active systems due to their reduced mechanical complexity and failure modes [1]. While active cooling designs rely on the pumping of coolant to remove heat from the reactor and maintain safe operating temperatures via forced convection, passive cooling relies on natural convection induced by temperature gradients in the coolant. Accordingly, the effective modeling and design of passively cooled reactor systems is dependent on accurate physical modeling of natural convection [2].

Current Gen IV reactor concepts include gas-cooled, water-cooled, and salt-cooled designs. Molten salt reactors (MSRs) are a promising concept due to their ambient operating pressures, eliminating the need for expensive pressure vessels, and ability to burn a broad range of fuels including existing nuclear waste [1]. However, the physics of natural convection at high temperature in molten salts remains an area of active research and further work is required to ensure accurate heat transfer modeling for reactor design.

*Corresponding Author
E-mail address: noah.lefrancois@mail.mcgill.ca

Empirical correlations are a powerful tool for predicting convective heat transfer rates in a broad range of fluids, and are widely used in the design of heat transfer systems. While much of the early work on empirical correlation measurement was conducted on water and air [3] [4], this data has been found to be applicable to a wide range of heat transfer fluids [5] [6]. Such methods have even been found to be applicable to forced and mixed convection problems in molten nitrate salts [7]. However, a recent study by Yu et al. [8] suggested that existing correlations may overestimate heat transfer rates for turbulent natural convection in a low-temperature eutectic mixture of $LiNO_3$-$CaNO_3$-$NaNO_3$-KNO_3. This result suggests that further work is required to provide reliable data for heat transfer rates in various molten salt mixtures of interest across a range of Rayleigh numbers.

In this work, we present measurements of the Nusselt number for a eutectic mixture of NaNO3-KNO3 (commonly known as Solar Salt) in a differentially-heated rectangular cavity for Rayleigh numbers ranging from 10^7 - 10^8.

2. NATURAL CONVECTION IN ENCLOSURES

Turbulent natural convection in enclosures is a well-studied phenomenon, with important applications to passive cooling systems and thermal energy storage. Early work in this area includes studies of heat transfer rates in a horizontal layer of water by Chu & Goldstein and Garon & Goldstein, finding that the Nusselt number could be modeled by a power law function of the Rayleigh number for Ra between 10^5 and 10^9 [3] [4]. Globe & Dropkin studied heat transfer rates in silicone oil and mercury in addition to water, and examined the dependence of the Nusselt number on both the Rayleigh and Prandtl numbers [5]. This study found a similar Ra dependence to the aforementioned studies of water and also found that the Nusselt number was proportional to $\mathrm{Pr}^{0.074}$. In general, heat transfer correlations for natural convection in horizontal enclosures can be expressed in the form of Eq. 1 [6] [9]:

$$\mathrm{Nu}(\mathrm{Ra}, \mathrm{Pr}) = C\mathrm{Ra}^n\mathrm{Pr}^m \tag{1}$$

A summary of the correlations proposed by the above studies, along with the parameter ranges examined in each study, is given in Table 1. The fit coefficients observed in the present study, discussed in Sec. 4, are also listed for comparison.

While there is generally good agreement between the above studies using water, air, and other common engineering fluids such as thermal oils, few studies have been performed to demonstrate their applicability to molten salts, which have significantly higher operating temperatures and Pr than these other fluids. Bin et al. studied the applicability of existing correlations to turbulent forced convection of molten lithium nitrate for $2\times10^4 < \mathrm{Re} < 5\times10^4$ and $12.7 < \mathrm{Pr} < 14.7$ [7]. This data showed good agreement with various correlations including those of Sieder-Tate, Petukhov, and Hausen, suggesting that existing correlations can be used for modelling forced convection of molten nitrates. However, Yu et al. found that existing correlations including those of Chu & Goldstein, Garon & Goldstein, and Globe & Dropkin significantly over-predict the Nusselt numbers observed for natural convection of a low-temperature nitrate eutectic mixture at $7\times10^7 < \mathrm{Ra} < 1.2\times10^9$ and $22 < \mathrm{Pr} < 30$ [8]. The authors proposed a new correlation based on this data, shown in Table I, which is dependent only upon Ra.

Table I. Nusselt correlations

Reference	Fluid	Ra	C	n	m
Garon & Goldstein	water	$1.3 \times 10^7 < \text{Ra} < 3.3 \times 10^9$ $5 < \text{Pr} < 7$	0.130	0.293	0
Chu & Goldstein	water	$2.8 \times 10^5 < \text{Ra} < 1.1 \times 10^8$ $5.5 < \text{Pr} < 6.5$	0.183	0.278	0
Globe & Dropkin	water, silicone oil, mercury	$1 \times 10^5 < \text{Ra} < 7 \times 10^8$ $0.02 < \text{Pr} < 8750$	0.069	0.333	0.074
Yu et. al	$LiNO_3$-$CaNO_3$-$NaNO_3$-KNO_3	$7 \times 10^7 < \text{Ra} < 1.2 \times 10^9$ $22 < \text{Pr} < 30$	0.0445	0.308	0
Current Work	$NaNO_3$-KNO_3	$2 \times 10^7 < \text{Ra} < 2 \times 10^8$ $5 < \text{Pr} < 12$	0.068	0.308	0.147

3. EXPERIMENTAL PROCEDURE

3.1. Experimental Setup

Fig. 1 shows the schematic diagram of the experimental setup. An alumina ceramic crucible is filled with salt and heated from below, with the top of the crucible open so that the top surface of the salt will be cooled by the surrounding air. A custom heater was designed to provide a maximum power of 1500 W at temperatures up to 800 °C; this heater consists of a steel plate which encloses a radiative heating panel in order to provide a uniformly heated surface on which to place the crucible. The crucible and heater are insulated with 15 cm of high-temperature ceramic fiber thermal insulation in order to reduce heat losses to the surroundings and create adiabatic side wall boundary conditions for the cavity.

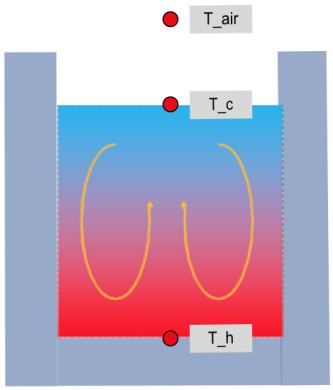

Figure 1. Schematic diagram of experimental setup for natural convection of molten salt.

The temperature at the heated bottom surface of the salt, T_h, was measured directly using a thermocouple inserted from the open crucible top and placed in contact with the bottom crucible surface. Type K ther-

mocouples from Omega Engineering were used, with an accuracy of max(2.2 °C, 0.75%) specified by the manufacturer.

Reliable and precisely repeatable measurement of the temperature, T_c, of the exposed top surface of the salt using a thermocouple positioned at the salt surface was challenging since the salt height was varied significantly between measurements. Instead, T_c was measured using a FLIR A700 IR camera. An example of this data is shown in Fig. 2. Note that the thick line of low temperatures is due to the thermocouple used to measure T_h, as labelled in the figure. The measured value of T_c was taken as the average temperature of a 0.25 cm x 0.25 cm square region in the centre of the surface, chosen to match the spatial resolution of the T_h thermocouple measurement. The uncertainty on this measurement was specified by the manufacturer as max(2 °C, 0.75%).

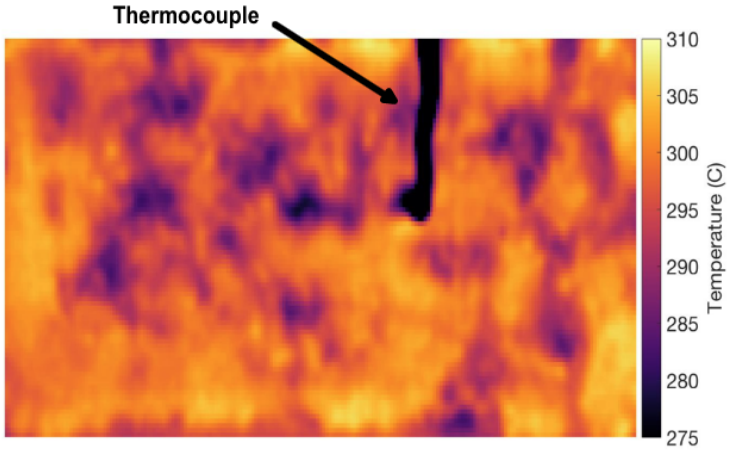

Figure 2. IR camera measurement of salt top surface temperature.

3.2. Experimental Data Analysis

The flux passing through the salt from the heated bottom wall, Q_s, is difficult to obtain via measurements of the heater power or hot plate temperature distribution due to imperfect insulation of the heater and unknown contact resistances between the heater and crucible. While the heater and crucible are wrapped in approximately 15cm of ceramic fiber thermal insulation on all sides to provide adiabatic boundary conditions for the crucible side walls, the fraction of the heater input power which reaches the bottom wall of the crucible and passes through the salt is still difficult to determine with the required accuracy for the intended data analysis due to the high heater temperatures and small surface area of the crucible bottom compared to the total surface area of the insulated setup.

Instead, the value is calculated by assuming that heat losses through the crucible side walls can be neglected and that 100% of the flux through the salt leaves through the exposed top surface. Given this assumption, we can evaluate Q_s by calculating the heat lost to the surroundings through the top surface of the salt.

Q_s is assumed to consist of two components: the convective losses from the top surface, Q_{conv}, and the radiative losses from the top surface, Q_{rad}. Q_{conv} is calculated according to Eq. 2, which uses the correlation for a horizontal plate cooled from above given by Cengel & Ghajar, $\mathrm{Nu} = 0.59\mathrm{Ra}^{1/4}$ [9].

$$Q_{conv} = hA\Delta T \tag{2}$$

Q_{rad} is evaluated using a gray surface-to-surface radiation model. The problem geometry is shown in Fig. 3, and the resistance network model used to solve for Q_{rad} is shown in Fig. 4. The temperature of the wall used for surface 2 is assumed to be equal to the average salt surface temperature used for surface 1, while the temperature of the surroundings used for surface 3 is measured using a thermocouple suspended 30 cm above the crucible. The surface emissivities of the salt was taken as $\epsilon_1 = 0.9$ [10], while the wall emissivity was taken as $\epsilon_2 = 0.25$ [11]. Surface 3 was assumed to be a blackbody with $\epsilon_3 = 1.0$.

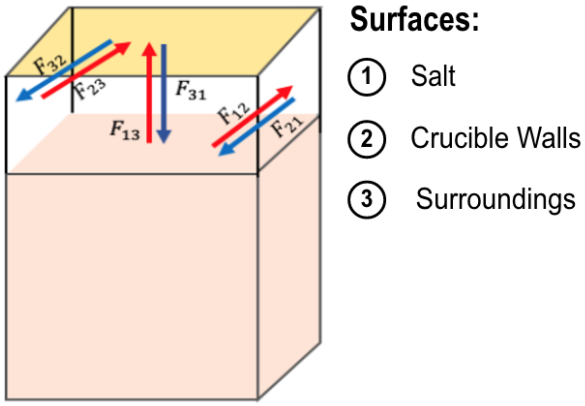

Figure 3. Geometry of surface-to-surface radiation problem for losses from salt surface. Salt (surface 1) shown in pink, exposed crucible walls (surface 2) shown in white, and crucible opening to surroundings (surface 3) shown in yellow.

The problem of calculating the flux Q_{rad} leaving the salt surface can be modeled as gray surface-to-surface radiation in a three-surface enclosure and solved by constructing the equivalent thermal resistance network according to Eq. 13-41 of Cengel & Ghajar [9]. The equivalent thermal resistance network is shown in Fig. 4; $Q_{rad} = Q_1$ is obtained by solving for the fluxes Q_1,Q_2,Q_3 which satisfy the condition that the algebraic sum of the currents at each node (highlighted in red) must equal zero.

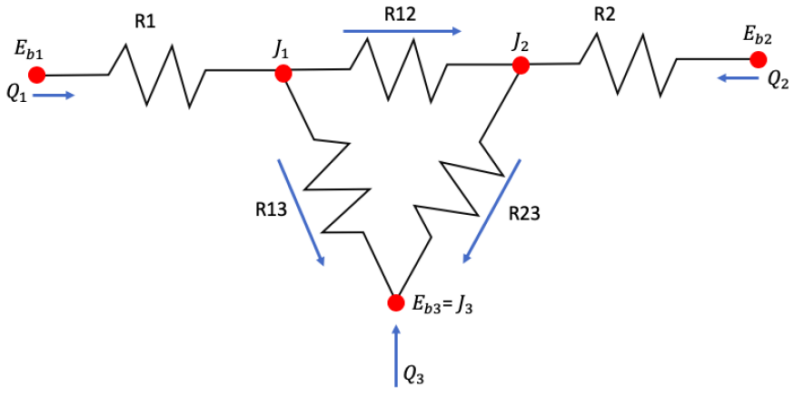

Figure 4. Equivalent resistance network for radiative exchange between salt surface, crucible walls, and surroundings.

Once Q_s has been obtained by summing the contribution of the convective and radiative losses calculated above, the Nusselt number is calculated according to Eq. 3:

$$\text{Nu} = \frac{Q_s L_c}{kA\Delta T} \tag{3}$$

where L_c is the characteristic length scale of the flow. For the rectangular cavity under consideration, L_c is equal to the height of the salt layer. ΔT is equal to the difference between T_h and T_c, while A is the cross-sectional area of the salt layer and k is the thermal conductivity of the salt.

With these measurements of T_h, T_c, and Q_s, we can calculate the Ra, Pr, and Nu values for each data point and perform a non-linear least squares fit to find a correlation of the form given in Eq. 1.

4. RESULTS & DISCUSSION

Preliminary data displaying the relationship between Nu and Ra is shown in Fig. 5. The correlations of Globe & Dropkin, Garon & Goldstein, and Yu et al. are displayed alongside the data for comparison. This data agrees well with the correlation of Garon & Goldstein, in contrast to the significantly lower values of Yu et al. This discrepancy may be due to significant differences in the Prandtl number range studied by Yu et al., as their $LiNO_3$-$CaNO_3$-$NaNO_3$-KNO_3 salt mixture has Prandtl numbers between 22-30 at the temperatures tested, while the $NaNO_3$-KNO_3 mixture studied in the present work has Prandtl numbers between 5-12, much closer to the range of Prandtl numbers seen in experiments with water.

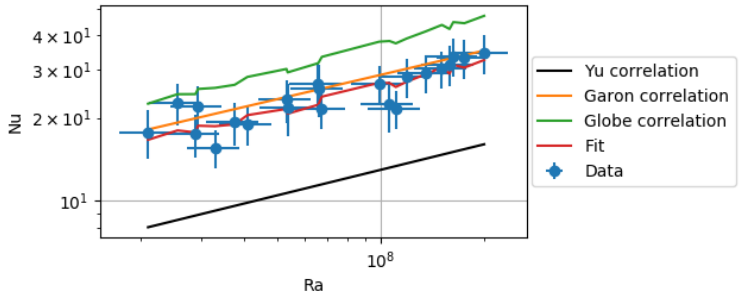

Figure 5. Dependence of heat transfer rates on Rayleigh number for experimental data and empirical correlations. Yu et al. correlation, Garon & Goldstein correlation, and Globe & Dropkin correlation are shown alongside a least-squares fit of the data.

The correlation of Globe & Dropkin as well as the fit to the present data both display non-monotonicity with increasing Rayleigh number in Fig. 5. This is due to the Nusselt number depending on both the Rayleigh number and the Prandtl number, which is not displayed explicitly on these 2D axes. Fit values for the data are found to be C = 0.068, n = 0.308, and m = 0.147. The Rayleigh dependence given by n lies within the range of other correlations shown in Table I, which are all near or slightly below 1/3. The prefactor C has a value about 1.5 times larger than proposed by Yu et al. as displayed by the significantly lower Nusselt number predictions of that correlation compared to the present data despite their identical Rayleigh dependence.

A non-negligible Prandtl number dependence is also indicated by the fit value of m. While Prandtl number dependence was not studied by Yu et al., these findings suggest that it is an important variable to include in Nusselt number correlations intended for use in the design of molten salt systems. This is especially relevant in light of the numerous molten salt mixtures under consideration for use as fuel-carriers, coolants, and thermal energy storage media in molten salt nuclear reactor designs, which can display widely varying thermophysical properties [12], [13], [14].

Based on these findings, continued experimental work is being undertaken to extend the Nusselt number measurements to a wider range of Rayleigh and Prandtl numbers in order to establish the range of validity of the present correlation coefficients. Using the apparatus and analysis methods presented here, these measurements can be repeated for a variety of molten salt mixtures and cavity sizes. This will improve the information available for the design and analysis of heat transfer systems which rely on natural convection of molten salt.

4.1. Uncertainty Analysis

Error bars for the data points displayed in Fig. 5 are estimated based on the propagation of uncertainties on the measured quantities used to calculate Nu. These quantities include the salt temperatures T_h and T_c, the air temperature T_a, and the material properties obtained from literature values. The thermophysical properties for solar salt reported by the salt supplier were assumed to have an uncertainty of 10% [15]. The salt surface emissivity reported by [10] was also assumed to have an uncertainty of 10%.

In order to identify major sources of uncertainty in our results, the contributions of each measured or ref-

erenced quantity to the overall uncertainty on the derived quantities Ra, Pr, Q_s, and Nu was evaluated and displayed in Fig. 6. The individual contribution of each source to the total uncertainty on the derived value was calculated by setting the uncertainty of all other sources to zero and evaluating the model for the derived quantity and its uncertainty. This uncertainty was then normalized by the value of the derived quantity. The results of this analysis indicate that the uncertainty on the thermophysical properties of the molten salt mixture and the measurement uncertainty on T_c are the largest contributors to the uncertainty of the derived quantities. The total uncertainty was found to be approximately 2% for Pr, 14% for Ra, 10% for Q_s, and 16% for Nu.

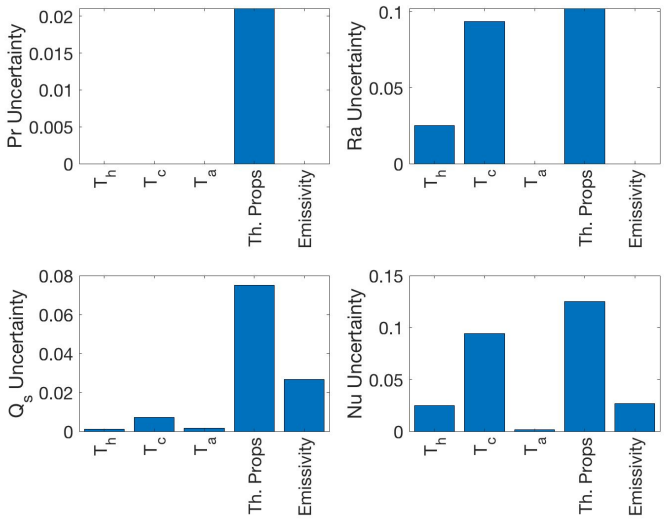

Figure 6. Contributions of measurement uncertainties (T_h, T_c, T_a) and material property uncertainties (thermophysical properties and emissivity of salt) to the propagated uncertainties on derived quantities. Uncertainties for each derived quantity have been normalized by the value of the derived quantity.

5. CONCLUSIONS

By investigating the relationship between the Nusselt and Rayleigh numbers in a differentially-heated cavity, a comparison of heat transfer rates in molten nitrate salt to the predictions of widely-used empirical correlations has been performed. A comparison between data obtained with $NaNO_3$-KNO_3 for $2x10^7 < Ra < 2x10^8$, $5 < Pr < 13$ and correlations obtained via measurements of water and other low-temperature fluids shows that these existing correlations provide accurate predictions of Nusselt number measurements in this range, despite Nusselt number data from a $LiNO_3$-$CaNO_3$-$NaNO_3$-KNO_3 mixture at higher Prandtl number having been found to be lower by a factor of 2 [8]. This suggests that further work is required to ensure confidence in the accuracy and range of applicability of Nusselt number correlations in order to inform the design of molten salt systems in advanced reactor technologies. This improved understanding of the variables affecting heat transfer rates in molten nitrate salts will contribute to the accurate modeling of molten salt thermal hydraulics, with important applications to the design of passive cooling systems in molten salt reactors.

ACKNOWLEDGMENTS

This work was supported by the Natural Sciences and Engineering Research Council of Canada (NSERC), funding reference number RGPIN-2019-05845, and the Fonds de recherche du Québec – Nature et technologies (FRQNT), funding reference 2022-NC-298727. The authors would also like to thank Sociedad Química y Minera (SQM) for donating the nitrate salts.

REFERENCES

1. T. Dolan, *Molten Salt Reactors and Thorium Energy* (2017).
2. P. Rubiolo, M. Retamales, V. Ghetta, and J. Giraud, "High temperature thermal hydraulics modeling of a molten salt: application to a molten salt fast reactor (MSFR)," *ESAIM: Proceedings and Surveys*, **58**, pp. 98–117 (2017); https://doi.org/https://doi.org/10.1051/proc/201758098.
3. T. Chu and R. Goldstein, "Turbulent convection in a horizontal layer of water," *Journal of Fluid Mechanics*, **60**, pp. 141–159 (1973).
4. A. Garon and R. Goldstein, "Velocity and heat transfer measurements in thermal convection," *The Physics of Fluids*, **16** (1973); https://doi.org/https://doi.org/10.1063/1.1694219.
5. S. Globe and D. Dropkin, "Natural Convection Heat Transfer in Liquid Confined by Two Horizontal Plates and Heated From Below," *Journal of Heat Transfer*, **81**, pp. 24–30 (1959).
6. W. Rohsenow, J. Hartnett, and Y. Cho, *Handbook of Heat Transfer*, McGraw-Hill (1998).
7. L. Bin, W. Yu-ting, M. Chong-fang, Y. Meng, and G. Hang, "Turbulent convective heat transfer with molten salt in a circular pipe," *International Communications in Heat and Mass Transfer*, **36**, pp. 912–916 (2009); https://doi.org/10.1016/j.icheatmasstransfer.2009.06.003.
8. Q. Yu, Y. Lu, C. Zhang, Y. Wu, and B. Sunden, "Experimental and numerical study of natural convection in bottom-heated cylindrical cavity filled with molten salt nanofluids," *Journal of Thermal Analysis and Calorimetry*, **141**, pp. 1207–1219 (2020); https://doi.org/https://doi.org/10.1007/s10973-019-09112-9.
9. Y. Cengel and A. Ghajar, *Heat and Mass Transfer: Fundamentals Applications*, McGraw-Hill (2015).
10. M. Tetreault-Friend, L. Gray, S. Berdibek, T. McKrell, and A. Slocum, "Optical properties of high temperature molten salt mixtures for volumetrically absorbing solar thermal receiver applications," *Solar Energy*, **153**, pp. 238–248 (2017); https://doi.org/http://dx.doi.org/10.1016/j.solener.2017.05.054.
11. M. Schalles and G. Blumroder, "Calculation of the effective emissivity of blackbodies made of alumina," *Measurement Science and Technology*, **23** (2012).
12. A. Caraballo, S. Galan-Cadado, A. Caballero, and S. Serena, "Molten salts for sensible thermal energy storage: a review and an energy performance analysis," *Energies*, **14** (2021); https://doi.org/https://doi.org/10.3390/en14041197.
13. W. Ding, A. Bonk, and T. B. and, "Molten chloride salts for next generation CSP plants: Selection of promising chloride salts study on corrosion of alloys in molten chloride salts," *AIP Conference Proceedings*, **2126** (1), pp. 200014 (2019); https://doi.org/10.1063/1.5117729.
14. M. Sohal, M. Ebner, P. Sabharwall, and P. Sharpe, "Engineering Database of Liquid Salt Thermophysical and Thermochemical Properties," Report, Idaho National Laboratory (2013).
15. SQM, "Sociedad Química y Minera's Thermo-Solar Salts," 2018.